Available online at www.sciencedirect.com

ScienceDirect

Procedia Engineering 70 (2014) 545 – 554

Procedia Engineering

www.elsevier.com/locate/procedia

12th International Conference on Computing and Control for the Water Industry, CCWI2013

Algorithms for automatic, real-time tsunami detection in wind-wave measurements: using strategies and practical aspects

M. Di Risio[a,*], G.M. Beltrami[a]

[a] *University of L'Aquila, Civil, Dep. Construction-Architectural and Environmental Engineering, Environmental and Maritime Hydraulic Laboratory, P.le Pontieri 1, 67040 Monteluco di Roio, L'Aquila, Italy*

Abstract

The present paper concentrates on the actual use - in the framework of a Tsunami Early Warning System - of the algorithms to be implemented in the software of wind-wave gages in order to automatically perform the real-time detection of tsunamis within recorded signals. Focus is on the amplitude-discriminating algorithm, mainly based on an infinite impulse response time domain filter, proposed by the authors in a previous paper. In particular, the problems that may arise in filtering out 'disturbances' such as long tidal waves are addressed, and an original method to perform the full characterization of the waveform of an actually detected tsunami, automatically and in 'quasi' real-time is proposed. Tests were carried out using time-series resulting from the superposition of actual tsunami signals recorded by some of the tsunamometers of the Deep-ocean Assessment and Reporting of Tsunamis program, and different wind-wave signals synthesized by means of the random-phase method. In particular, the tsunamometers' records collected during the events triggered by the earthquakes occurred off the coast of Chile on February 27, 2010, and off the Pacific Coast of Tohoku (Japan) on March 11, 2011, were used. The results show that the overall detection and characterization of a tsunami can be effectively carried out, automatically and in real-time, using the proposed new algorithm.

Selection and peer-review under responsibility of the CCWI2013 Committee

Keywords: Tsunami detection algorithm; real-time; filtering techniques; tsunami early warning systems

1. Introduction

Although tsunamis may be generated by either earthquakes, or coastal landslides (either submerged or subaerial), or eruptions of submerged volcanoes, or meteorites impacting the ocean, the most frequent generating events are by far earthquakes. Due to this reason, the main Tsunami Early Warning Systems (TEWSs) actually operating around the world usually rely on seismic monitoring of probable tsunami sources in order to perform a fast detection of possible tsunamigenic earthquakes and to issue rapid initial warnings. On the other hand, a ground-movement monitoring network should be included as part of a TEWS oriented at issuing early warning of tsunamis generated by landslides (e.g. Di Risio et al., 2011). By way of example, following the tsunamis generated on December 30, 2002 by landslides

* Corresponding author. Tel.: +39-(0)862-434534 ; fax: +39-(0)862-434554.
E-mail address: marcello.dirisio@univaq.it

Selection and peer-review under responsibility of the CCWI2013 Committee
doi:10.1016/j.proeng.2014.02.060

detached from the north-west flank of the volcano of Stromboli (e.g. Tinti et al., 2003, Di Risio et al., 2009a, De Girolamo et al., 2011), the 'Dipartimento della Protezione Civile', DPC (Italian Civil Protection Department), sets up a specific TEWS which relies primarily on real-time monitoring of both the volcano seismic activity (e.g. Langer and Falsaperla, 2003), and the 'Sciara del Fuoco' ground movements (e.g. Corsini et al., 2006, Casagli et al., 2010).

Whatever the criterion used by a TEWS for issuing rapid initial warnings, it is to be stressed that, in spite of the great effort recently undertaken by the scientific and engineering community in developing new technologies (e.g. satellite altimetry, detectors of low-frequency elastic oscillations associated to a tsunami, e.g. Hamlington et al. 2011, Chierici et al. 2010, Sammarco et al. 2013) capable of increasing the awareness of a potential tsunami in the minimum amount of time, at present only direct detection in sea-level measurements can confirm its actual generation and propagation (e.g. Bellotti et al., 2009, Bressan and Tinti, 2011, 2012). The sea-level measurement network and the algorithms used to perform such an automatic, real-time detection are therefore main components of a TEWS.

Aside from the accelerometer-based floating buoys, wind-wave gauges (WWGs) equipped with either pressure, or acoustic, or optical sensors are inherently poly-functional devices capable of detecting not only wind and infra-gravity waves, but also tides and tsunamis. Clearly, the detection algorithm to be implemented in the software of a WWG should be capable of discriminating a tsunami from other sea-level oscillations that, falling within the frequency band detected by the sensor, are 'disturbances' in the context of tsunami detection. Only filtering out these 'disturbances' (i.e. mainly wind-waves and tides) makes it possible to monitor the actual propagation of a tsunami by checking either the amplitude or the slope of the filtered signal against a prescribed threshold.

At present, the only algorithms expressly designed to detect a tsunami in real-time within a WWG recorded signal are that developed by McGehee and McKinney (1995), and that used by the DPC within the Stromboli's TEWS Leva (2004). Both these algorithms are based on time-domain moving-average filters, also known as running-mean filters. A further algorithm Shimizu et al. (2006), that relies on a finite impulse response (FIR) time domain filter (TDF), has been proposed by the Port and Airport Research Institute of Japan (PARI) for the automatic, real-time detection of a tsunami in the sea-level measurements collected by the Doppler typed Wave Directional Meter (DWDM) and the GPS buoys of the Japanese Nationwide Ocean Wave information network for Ports and HArbourS (NOWPHAS). More recently Beltrami and Di Risio (2011) proposed an amplitude-discriminating algorithm based on the use of infinite impulse response (IIR) time domain digital filter (TDF).

The present paper concentrates on the actual use (in the framework of a Tsunami Early Warning System) of the algorithms to be implemented in the software of WWGs in order to automatically perform the real-time detection of tsunamis within recorded signals. Focus is on the amplitude-discriminating algorithm presented by Beltrami and Di Risio (2011). In particular, the paper addresses the problems that may arise in filtering out disturbances such as long tidal waves, and presents an original method to perform the full characterization of the waveform of an actually detected tsunami, automatically and in 'quasi' real-time. Tests were carried out using time-series resulting from the superposition of actual tsunami signals recorded by some of the tsunamometers of the Deep-ocean Assessment and Reporting of Tsunamis (DART) program, and different wind-wave signals synthesized by means of the random-phase method (Tuah and Hudspeth, 1982). In particular, the tsunamometers' records collected during the events triggered by the earthquakes occurred off the coast of Chile on February 27, 2010, and the Pacific Coast of Tohoku (Japan) on March 11, 2011, were used. The results of these tests show that the overall detection and characterization of a tsunami may be effectively carried out, automatically and in real-time, using the algorithm proposed by Beltrami and Di Risio (2011).

The paper is structured as follows. Form and characteristics of the algorithm proposed by Beltrami and Di Risio (2011) are briefly recalled in Section 2, illustrating the problems that may arise in filtering out 'disturbances' such as long tidal waves and their possible solutions (Sec. 2.3). An original method to perform the automatic, 'quasi' real-time characterization of the waveform of an actually detected tsunami is then presented in Section 3. The results of the overall tests carried out using the proposed algorithm are described and commented in Section 4, while observations are made and conclusions drawn in Section 5.

2. The algorithm by Beltrami and Di Risio (2011)

2.1. Standard tidal-wave module

The 'standard' form of the tidal-wave module (i.e. the module developed in order to filter out 'disturbances' such as the astronomical and meteorological tide) works as follows. Each new sample $\zeta(t_i)$ is stored in a vector $\{\zeta\}_i$ consisting of the samples collected during the last 3 h and 40 min. A modified version of the cubic polynomial on which relies the tsunami-detection algorithm developed by Mofjeld (1997) is then applied in order to filter out the tidal 'disturbance' from the signal $\{\zeta\}_i$. The modification consists in lengthening the time interval between the actual and the prediction time. In particular, the polynomial is fitted to p-minute averages $\bar{\zeta}$ (centered at the $p/2$ minute) of samples ζ stored over the 3 h and 10 min that precede of 30 min the current time. As shown by Beltrami (2011), the intent of such a lengthening (30 min in the present case) is that of delaying the moment at which a propagating tsunami influences the predictions by affecting the observation averages (in particular the first observation average). It is this delay that makes the filtered signal capable of giving a proper representation of tsunamis with period within the band 2-30 minutes, and therefore that makes the algorithm capable (automatically and in real-time) not only of detecting a tsunami but also of characterizing it in terms of amplitude and period.

Given the sampling frequency f_s, the output of the polynomial can be expressed as

$$\zeta_p(t_i) = \sum_{j=0}^{3} w_j \bar{\zeta}(t_{i-1800 f_s - 1} - 30p - 3600j) \tag{1}$$

where the coefficients w_j are calculated by applying the Newton's forward divided difference formula (Mofjeld, 1997, Beltrami, 2008, 2011). The tidal wave pattern is filtered out by subtracting at each new time step t_i the polynomial output $\zeta_p(t_i)$ from the corresponding sample $\zeta(t_i)$. The filtered sea-level at each new time step t_i is therefore expressed as $\zeta'(t_i)=\zeta(t_i)-\zeta_p(t_i)$.

2.2. Wind-wave module

As far as the wind-wave 'disturbance' is concerned the algorithm proposed by Beltrami and Di Risio (2011) works as follows. A vector $\{\zeta'\}_i=\{\zeta'(t_i),...,\zeta'(t_{i-n})\}_i$ consisting of the n samples spanning the time interval Δt_a is updated at each time step t_i. The signal stored in $\{\zeta'\}_i$ is lengthened using a fictitious series made of a transition signal $\{\zeta_t\}_i$ (of duration Δt_t) and by the mirror of $\{\zeta'\}_i$. The resulting signal is stored in the vector $\{\zeta''\}_i$ of duration $\Delta t=\Delta t_a+\Delta t_f$ (being $\Delta t_f=\Delta t_t+\Delta t_a$). A seventh order infinite impulse response (IIR) time domain digital filter (TDF), i.e.

$$\zeta'''(t_i) = \sum_{k=0}^{7} a_k \zeta''(t_{i-k}) - \sum_{h=1}^{7} b_h \zeta'''(t_{i-h}), \tag{2}$$

is then applied in order to perform the *bidirectional* filtering of all the samples contained in vector $\{\zeta''\}_i$. The filter taps are calculated *once and for all* and *a priori* for a given frequency band pass.

It is also useful to recall that the IIR-TDF uses the Butterworth (1930) approximation of the gain or magnitude response function (e.g. Smith, 1997, Emery and Thomson, 2001, Shenoi, 2006, Goring, 2008), and that a bidirectional filtering (e.g. Smith, 1997) of the considered signal segment has to be applied in order to avoid an output phase shift. The results of the combination of forward and reverse filtering are stored in vector $\{\zeta'''\}_i$. The filtered sample at time t_i, is then extracted from $\{\zeta'''\}_i$ and stored in a further vector $\{\zeta^*\}_i = \{\zeta'''(t_i),...,\zeta'''(t_{i-r})\}_i$, consisting of the $(r-1)$ values obtained in the last r/f_s seconds. At each new time step t_i, the sea-level sample $\widehat{\zeta}(t_i)$ filtered for the 'disturbance' due to wind-waves is finally obtained by taking the mean $\overline{\zeta^*}_i$ of $\{\zeta^*\}_i$. A tsunami will be triggered if $|\widehat{\zeta}(t_i)|$ exceeds a preselected threshold TS_{amp}.

The application of the described module implies a choice for the values of parameters such as the duration of time intervals Δt_a, Δt_t and the number r of samples stored in vector $\{\zeta'''\}_i$. This choice clearly depends on the range of periods of the tsunamis to be detected. By way of example, Tab. 1 shows the values chosen in order to give the algorithm the wider range of application, i.e. in order to make the algorithm capable of detecting tsunamis with periods larger than 60 s.

Table 1. Values for the algorithm parameters suggested in the case of a sampling frequency equal to 2 Hz.

parameter	*value*	*units*
Δt_a	30	minutes
Δt_t	6	s
r	45	samples

2.3. Tidal-wave filtering: problems and solutions

Choosing the modified version of the cubic polynomial used by Mofjeld (1997) has the appealing pro of making the overall algorithm site independent. In-fact, as the taps of the IIR-TDF (see Section 2.2), the coefficients w_j in Eq. (1) are calculated *once and for all* and *a priori* and therefore do not depend on the location of the measurement device. Nevertheless, as shown by Beltrami (2011), the modification of the prediction time setting, while makes possible the contemporaneous detection and characterization of a tsunami, affects the algorithm performance in filtering out tidal waves at locations characterized by a high tidal range. The prediction error of the cubic polynomial, and therefore the departure from a perfectly filtered signal (a zero signal in the case of absence of tsunami), actually depends both on the time interval p and on the range of the tide to be filtered out. Given an averaging interval p=10 min, the filtered signals obtained by testing the polynomial on M_2 tides of equal phase and different amplitudes show a residual oscillation of sinusoidal shape (Beltrami, 2008, 2011). The longer the prediction time interval, the greater the range of this residual oscillation. By way of example, when the prediction time is set equal to 0.25 min with respect to the actual time, the range of this oscillation will be approximately 0.3 % of the tidal one. On the other hand, if the prediction time is set equal to 30.25 min, the range of this oscillation will be approximately 2.6 % of the tidal one (Beltrami, 2011), i.e. an order of magnitude greater than in the case of prediction time set equal to 0.25 min. Therefore, a residual oscillation of few centimeters may still be present in the filtered signal at a location that experiences a high tidal range. In this case, the detection threshold should be augmented of the amplitude of such a persisting oscillation. Consequently, the amplitude of the lower detectable tsunami is augmented and the detection performance of the algorithm reduced. However, from a practical point of view, such a reduction does not influence the overall efficiency of the algorithm. In-fact, the lower the water depth, the higher the expected amplitude of an actually threatening tsunami. By way of example, the water depth at the location of a fixed offshore platform (i.e. one of the deepest structures on which a WWG can be mounted) generally varies between several tens to some hundreds of meters. At such a water depth the amplitude of an actually threatening tsunami is expected to be several tens of centimeters or more, i.e. a value that cannot be masked by the residual oscillation.

In any case, another option will be available if a high detection performance is necessary. This option consists in using the original version of the cubic polynomial as devised by Mofjeld (1997), i.e. with prediction time set equal to 0.25 min with respect to the actual time. In this case, the overall algorithm is capable of detecting a propagating tsunami but not of characterizing it in real-time (Beltrami, 2011). Such a characterization can be carried out in ‘quasi’ real-time using the method illustrated in the next Section. Moreover, if the main issue is that of both detecting and characterizing a tsunami in real-time and that of keeping the threshold as lower as possible, two further alternatives will be available at the condition of accepting site-dependency: (i) the implementation of a varied version of the artificial neural network (ANN) proposed by Beltrami (2008, 2011); and (ii) the use of the harmonic prediction of the astronomical tide (corrected for the meteorological one) as done by Shimizu et al. (2006) in the algorithm by the Port and Airport Research Institute of Japan (see also, Beltrami and Di Risio, 2011). The reader is referred to the original papers for details on the implementation of these alternative methods.

3. Dynamic characterization of tsunami waveform, automatically and in ‘quasi’ real-time

The full characterization of the waveform of a propagating tsunami is essential for spreading the correct level of alarm. In-fact, such a waveform represents the initial condition to be used in the numerical models aimed at simulating the tsunami propagation toward the coasts at risk, and at forecasting the level of inundation (e.g. Bellotti et al., 2008, Cecioni and Bellotti, 2010a,b, Cecioni et al., 2011, Montagna et al., 2011).

The algorithm by Beltrami and Di Risio (2011) is capable not only of detecting, but also of characterizing the waveform of a tsunami propagating at a WWG location, automatically and in real-time. Nevertheless, it tends to

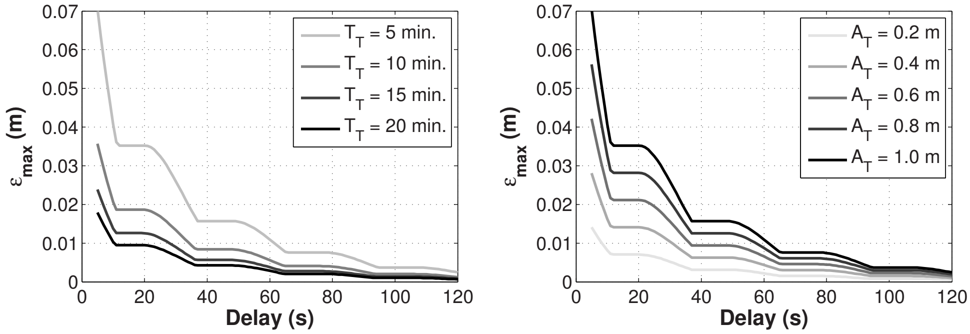

Fig. 1. Maximum value of synchronous error plotted against the time delay for varying tsunami period (left panel - tsunami amplitude equal to 1.0 m) and tsunami amplitude (right panel - tsunami period equal to 5 min).

slightly underestimate the amplitude of such an anomalous wave. As shown by Beltrami and Di Risio (2011), this is mainly due to the mean $\overline{\zeta^*}_i$ that is taken of $\{\zeta^*\}_i$ in order to improve the filtering performance of the IIR-TDF (see also Section 2.2). In order to fully characterize the waveform of a tsunami, automatically and in 'quasi' real-time, the following method can be used once the tsunami is detected.

If the succession of overshoot ripples at both ends of the filtered signal (Gibbs, 1899, Beltrami and Di Risio, 2011) are no concern, nothing will prevent applying the IIR-TDF given in Eq. (2) directly to a vector $\{\zeta'\}$ of already collected and de-tided samples. Apart from these ends, the resulting filtered signal will show the waveform of the portion of any anomalous wave already present in this sample vector. Therefore, once a tsunami is detected, if the IIR-TDF is dynamically applied (at each new time step) to the correspondingly updated sample vector, the successive filtered signals will show the evolution of the tsunami waveform during its propagation. Clearly, such a characterization is performed in 'quasi' real-time, as a portion of the successive filtered signals close to the current time is not representative of the actual tsunami. In-fact, this portion is affected by the error due to the previously stated succession of overshoot ripples. The time interval corresponding to this portion represents a delay in the actual real-time characterization of the detected tsunami.

Introducing the *synchronous error*, i.e.

$$\varepsilon\left(t_i, \Delta t\right) = \left|\zeta_{TD}\left(t_i - \Delta t\right) - \zeta'''\left(t_i - \Delta t\right)\right|, \tag{3}$$

makes it possible to evaluate the performance of the proposed method of full characterization. The synchronous error is defined as a function of the current time t_i and the delay Δt, and gives the difference between the actual tsunami waveform $\zeta_{TD}(t)$ and the filtered signal $\zeta'''(t)$, i.e. the signal resulting from the application of one of the proposed de-tiding methods and the IIR-TDF given in Eq. (2). At each new time step, the collected sample vector is updated, and the corresponding portion of the actual tsunami present in this vector changes. Therefore, the filtered signal (and the synchronous error) changes accordingly. Finally, it is to be noticed that considering the *maximum synchronous error* as a function of Δt, i.e.

$$\varepsilon_{max}\left(\Delta t\right) = \max_{t_i}\left|\zeta_{TD}\left(t_i - \Delta t\right) - \zeta'''\left(t_i - \Delta t\right)\right|, \tag{4}$$

is particularly useful to get an estimate of the delay Δt between the detection and the full 'quasi' real-time characterization of a tsunami.

A series of simulations were carried out, using different synthetic time series, in order to evaluate the theoretical delay introduced in the real-time characterization of a detected tsunami. Each synthetic signal was obtained by superposing a different sinusoidal tsunami and the same wind-wave time series characterized by a significant wave height equal to 10.0 m and a peak period equal to 12.65 s. Given the aim of the tests, no tidal wave was considered. The filtered signal therefore consisted of only that resulting from the direct application of the IIR-TDF. The amplitude of the tsunami was varied within the range 0.2-1.0 m, while the period within the range 5-20 min. Fig. 1 shows the results of these simulations. In particular, the maximum synchronous error is plotted as a function of the delay

Δt, considering either different tsunami periods (left panel) or amplitudes (right panel). As it can be noticed, the lower the tsunami period (and the higher the tsunami amplitude), the larger the $\varepsilon_{max}(\Delta t)$. It is also to be noticed that the maximum synchronous error decreases as delay increases. In particular, $\varepsilon_{max}(\Delta t)$ is lower than 0.01 m for delays larger than about 60 s for all the tested tsunami parameters. The proposed method is therefore capable of fully characterize the waveform of a tsunami with a theoretical delay of about 1 min with respect to the actual time.

4. Application to (quasi-)real cases

Two sets of tests were carried out in order to asses the actual performance of the proposed algorithm and of the method of tsunami dynamic-characterization in the case of earthquake induced tsunamis. The records collected by two tsunamometers of the Deep-ocean Assessment and Reporting of Tsunamis (DART) program during the events triggered by the earthquakes occurred off the coast of Chile (February 27, 2010) and off the Pacific Coast of Tohoku (Japan, March 11, 2011) were considered in these cases. In particular, the analyzed signals resulted from the superposition of the actual tsunamometer's record (i.e. the tidal and tsunami component oversampled at a constant rate equal to 2 Hz), and different wind-wave time-series synthesized by means of the random-phase method (Tuah and Hudspeth, 1982).

4.1. Chilean tsunami: February 27, 2010

On February 27, 2010 a 8.8 Mw-magnitude earthquake occurred off the coast of the Chilean Maule Region. Following the earthquake, a tsunami was generated, propagating towards the Chilean coasts and radiating in the Pacific. The tsunami arrived at DART station 32412, located 630 nautical miles Southwest of Lima (Peru), around 09:40 UTC and reached its maximum amplitude (about 0.24 m over mean sea level) around 09:50 UTC (Beltrami, 2011). The signal collected by the tsunamometer of this station was selected as a first example of tsunami and tidal components embedded in the signal recorded by a WWG in the case of an earthquake generated tsunami. As only waves within the tsunami and tidal frequency band can be detected at the water depth of a tsunamometer (e.g. Beltrami, 2008), different randomly generated wind-wave signals were superimposed to the tsunamometer's record in order to obtain an almost real WWG signal. In particular, four wind-wave records, each characterized by a specific significant wave height (H_{m0} = 1, 4, 6, 10 m) and peak period ($T_p = 4\sqrt{H_{m0}}$, Goda, 2000), were considered.

The frequency characterization of the observed tsunami reveals that the upper bound of the band spanned by the tsunami frequencies is around $5 \cdot 10^{-3}$ Hz, corresponding to a period equal to 200 s. This bound is lower than the lower bound of the IIR-TDF pass-band. Therefore, the detection algorithm and method of characterization based on the IIR-TDF is expected to perform quite effectively.

A first set of tests was carried out on the signal resulting from the superposition of different wind-wave records and the tsunami record (being the tide previously filtered out). Fig. 2 (left) shows the actual tsunami waveform to be detected (dashed black line), along with the real-time filtered signal (black solid line) and the 'quasi' real-time filtered signal (gray solid line). This last signal was computed at 10:00 UTC of February 27 for all the considered wind-wave records. The vertical dash-dotted lines indicate the instant at which the alarm is spread, being the threshold set equal to 0.05 m. While the actual tsunami signal reaches the threshold at 9:44:45 UTC (theoretical alarm), the proposed detection algorithm allows to detect the tsunami at 9:45:23 UTC, i.e. with a delay of 38 s with respect to the theoretical alarm. It is to be noticed that the tsunami waveform is almost perfectly characterized in 'quasi' real-time. This is shown by the maximum synchronous error that is smaller than 0.01 m just after 10 s, and becomes almost negligible after about 30 s (see Fig. 4, left).

Fig. 2 (right) shows the results of the simulation carried out on the signal obtained superposing the original tsunamometer record and one of the wind-wave records (H_{m0} = 1.0 m). The upper panel shows the signal obtained filtering out wind waves, i.e. the signal resulting from the application of the sole wind-wave module. On the other hand, the signals resulting from the application of the tidal-wave module before and after the application of the wind-wave one are shown in the middle and lower panel respectively. As it can be noticed, the order of application of the modules does influence neither the real-time detection performance nor the 'quasi'-real-time characterization.

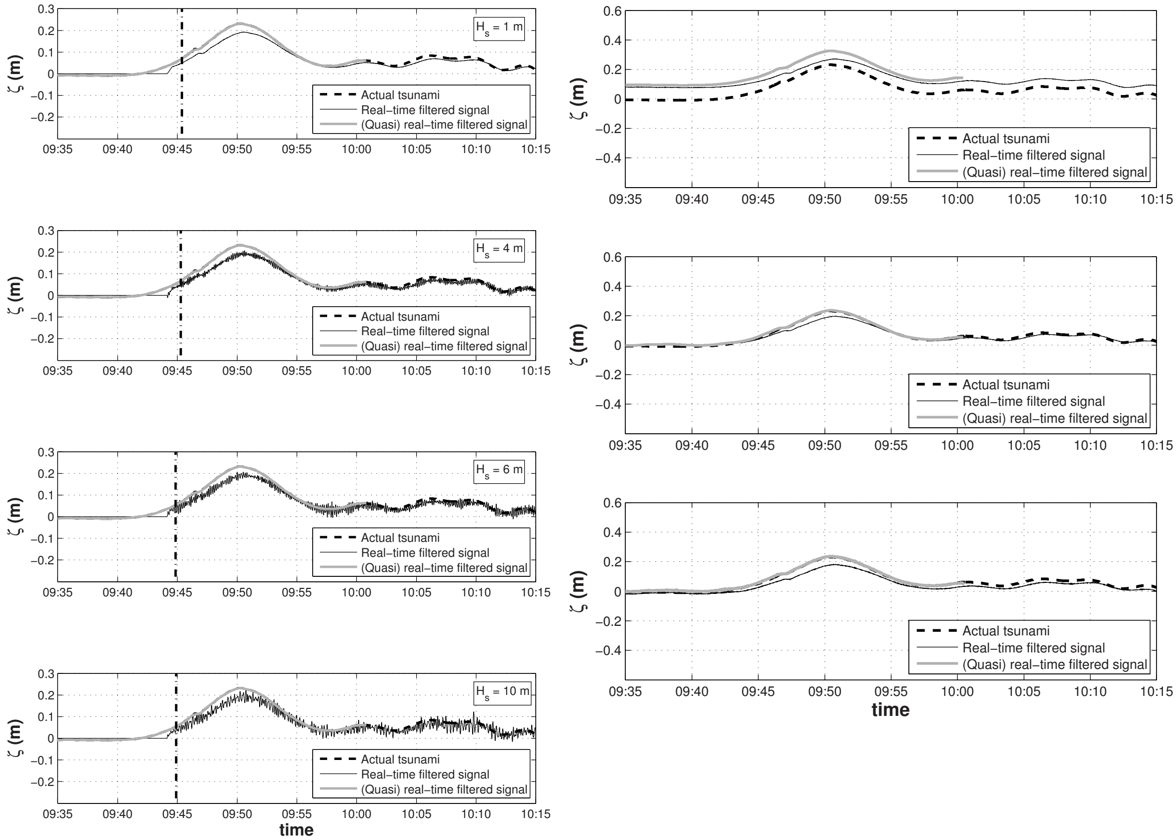

Fig. 2. *Left.* Actual tsunami waveform (dashed black lines), real-time filtered signal (solid black lines) and 'quasi' real-time filtered signal (gray solid lines) for all the considered short waves time series in the case of Chilean earthquake generated tsunami (February 27, 2010). The vertical dash-dotted black line indicates the instant of alarm for a threshold amplitude equal to 0.05 m. *Right.* Actual tsunami waveform in the case of Chilean earthquake generated tsunami (dashed black lines), real-time filtered signal (solid black lines) and 'quasi' real-time filtered signal (gray solid lines) for H_{m0} = 1.0 m without using of tidal module (upper panel), with using of tidal module before wave module (middle panel) and with using of tidal module after wave module (lower panel).

4.2. Japanese tsunami: March 11, 2011

As it is known, a devastating tsunami was generated by the 9.0 Mw-magnitude earthquake occurred off the coast of Sendai (Japan) at 05:46 UTC of March 11, 2011 ("The 2011 off the Pacific Coast of Tohoku Earthquake Tsunami"). The tsunami not only hit the overall North-East coast of Japan, but radiated in the Pacific reaching all its surrounding coasts. In-fact, it was detected by almost all the tsunamometers of the DART network and recorded by almost all the coastal tidal gauges. In particular, the tsunami arrived at DART station 51407, located 140 nautical miles Southeast of Honolulu (Hawaii, USA), around 13:25 UTC and reached its maximum amplitude (about 0.30 m over mean sea level) around 13:43 UTC. The signal collected by the tsunamometer of this station was selected as a second example of tsunami and tidal components. The same randomly generated wind-wave signals introduced in the previous section were then superimposed to the tsunamometer's record in order to obtain an almost real WWG signal. As in the previous case, the frequency characterization of the actual tsunami shows that the upper bound of the band spanned by the tsunami frequencies is lower than the lower bound of the IIR-TDF pass-band. Therefore, the detection algorithm (as well as the method of waveform characterization) based on the IIR-TDF is expected to perform quite effectively also in this case.

As in the previous case, a first set of tests was carried out on previously de-tided signals. Fig. 3 (left) shows the waveform of the actual tsunami to be detected (dashed black line), along with the real-time filtered signal (black solid

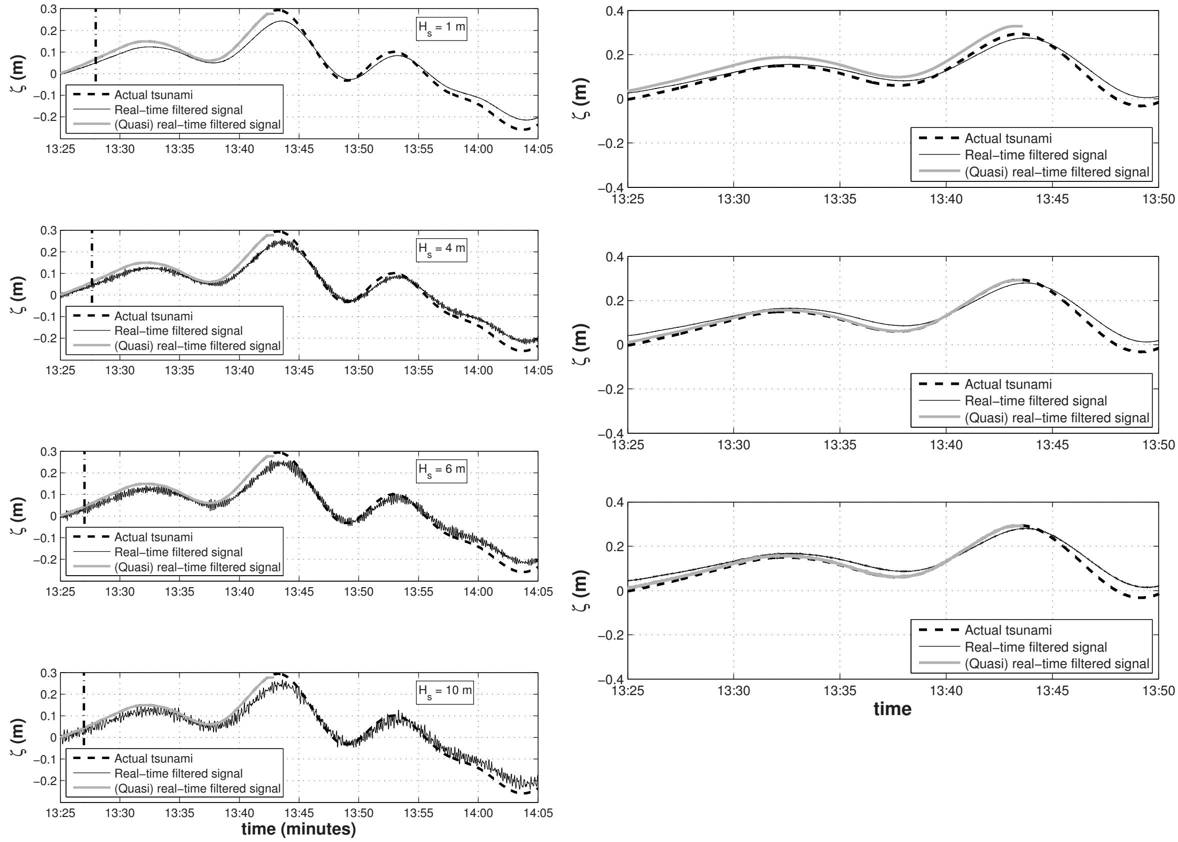

Fig. 3. As Fig. 2 in the case of Japanese earthquake generated tsunami (March 11, 2011).

line) and the ‘quasi’ real-time filtered one (gray solid line). This last signal was computed at 13:45 UTC of March 11 for all the considered wind-wave records. Theoretically, the alarm should be spread at 13:27:17 UTC, i.e. at the instant at which the amplitude of the actual tsunami reaches the assumed threshold (0.05 m). The proposed real-time detection algorithm allows to detect the tsunami and spread the alarm at 13:27:58 UTC (vertical dash-dotted lines), i.e. with a time delay of 41 s with respect to the theoretical alarm. Moreover, the tsunami waveform is almost perfectly characterized in ‘quasi’ real-time. As shown by Fig. 4, the maximum synchronous error drops below 1 cm just after about 10 s and becomes almost negligible after about 30 s. Such a result confirms that obtained in the case of the Chilean tsunami.

Fig. 3 (right) shows the results when tidal oscillations are retained in the input signal. As before, the upper panel shows the signal obtained filtering out wind waves, i.e. the signal resulting from the application of the sole wind-wave module. The signals resulting from the application of the tidal-wave module before and after the application of the wind-wave one are shown in the middle and lower panel respectively. It can be noticed again that the order of application of the modules does not influence the algorithm performance.

5. Concluding remarks and ongoing research

The present paper focused on the actual use of the algorithm proposed by the authors Beltrami and Di Risio (2011) and aimed at carrying out the automatic, real-time detection and characterization of a tsunami within the measurements collected by wind-wave gauges. The algorithm, mainly based on an infinite impulse response (IIR) time domain filter (TDF), belongs to the class of the amplitude-discriminating ones and - in its ‘standard’ form - is site-independent. A

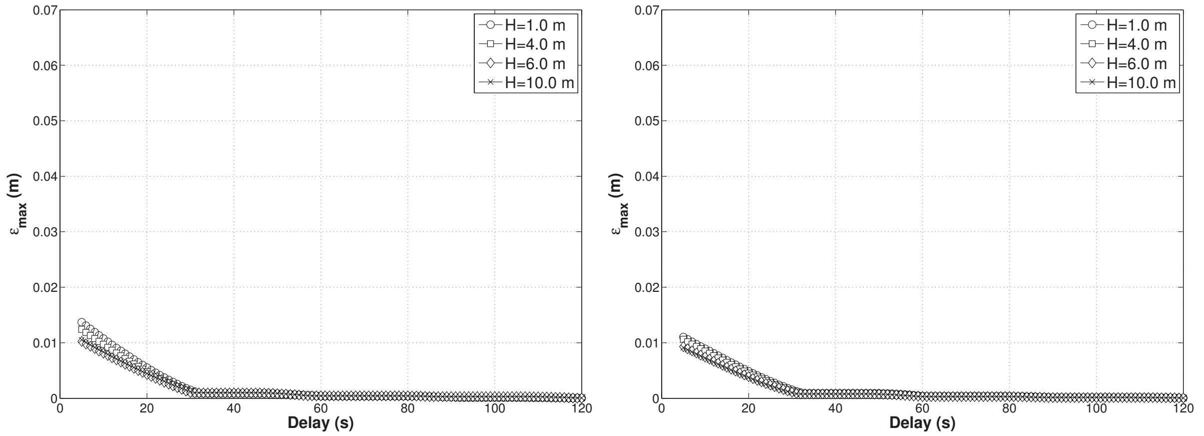

Fig. 4. Maximum synchronous error for varying significant wave height and time delay for the Chilean earthquake generate tsunami (right) and for the Japanese earthquake generated tsunami (right).

method to perform, automatically and in 'quasi' real-time, the full characterization of the tsunami waveform was also presented.

Two sets of tests were carried out in order to asses the actual performance of the proposed algorithm and of the method of tsunami full-characterization. The records collected by two tsunamometers of the Deep-ocean Assessment and Reporting of Tsunamis (DART) program during the events triggered by the earthquakes recently occurred off the coast of Chile (February 27, 2010) and off the coast of Japan (March 11, 2011) were considered and superposed wind-wave time series in order to synthesize a signal similar to that that might be recorded by a wind-wave gage (WWG).

The results of the tests confirm that the algorithm by Beltrami and Di Risio (2011) is capable not only of detecting, automatically and in real time, a tsunami propagating at a WWG location, but also of characterizing its waveform. As far as this method is concerned, the tests show that it is capable of an almost perfect characterization of the tsunami waveform, at least in the case of earthquake generated tsunamis.

Further research are in progress dealing with the application of the algorithm to real time series, also when other long components are present in the signals (i.e. edge waves, surf beats, etc...), in particular when the sensors are deployed close to the coast (e.g. Bellotti et al., 2012a,b).

6. Acknowledgments

This work was carried out under the research project PRIN2007 (prot. 2007MNBEMY) led by Prof. Paolo De Girolamo and funded by the Italian Ministry for University and Scientific Research (MIUR). Particular thanks are owed to Pr. Paolo De Girolamo for having encouraged the authors work, and his useful suggestions.

References

Bellotti G., Cecioni C., De Girolamo P., 2008 Simulation of small-amplitude frequency-dispersive transient waves by means of the mild-slope equation, Coastal Engineering, 55(6), 447-458 doi:10.1016/j.coastaleng.2007.12.006

Bellotti G., Di Risio M. and De Girolamo P., 2009. Feasibility of Tsunami Early Warning Systems for small volcanic islands. Natural Hazard and Earth System Sciences, Vol.9, 1911-1919.

Bellotti G., Briganti R., Beltrami G.M., Franco L. (2012a). Modal analysis of semi-enclosed basins. Coastal Engineering, vol. 64, p. 16-25.

Bellotti G., Briganti R., Beltrami G.M. (2012b). The combined role of bay and shelf modes in tsunamis amplification along the coast. Journal of Geophysical Research-Oceans, 117, C08027, doi:10.1029/2012JC008061.

Beltrami, G. M., 2008. An ANN algorithm for automatic, real-time tsunami detection in deep-sea level measurements. Ocean Engineering, 35(5-6), 572-587. doi:10.1016/ j.oceaneng.2007.11.009.

Beltrami, G. M., 2011. Automatic, real-time detection and characterization of tsunamis in deep-sea level measurements. Ocean Engineering, 38(14-15), 1677-1685. doi :10.1016/j.oceaneng.2011.07.016.

Beltrami G. M. and Di Risio M., 2011. Algorithms for automatic, real-time tsunami detection in wind-wave measurements. Part I: implementation strategies and basic tests. Coastal Engineering, 58(11), 10621071. doi:10.1016/j.coastaleng.2011.06.004

Bressan, L. and Tinti, S., 2011 Structure and performance of a real-time algorithm to detect tsunami 5 or tsunami-like alert conditions based on sea-level records analysis. Nat. Hazards Earth Syst. Sci., 11, 14991521, doi:10.5194/nhess-11-1499-2011, 2011. 2457, 2458, 2462, 2463, 2465, 2466

Bressan, L. and Tinti, S., 2012. Detecting the 11 March 2011 Tohoku tsunami arrival on sea-level records in the Pacific Ocean: application and performance of the Tsunami Early Detection Al10 gorithm (TEDA), Nat. Hazards Earth Syst. Sci., 12, 1583-1606, doi:10.5194/nhess-12-1583-2012, 2012. 2463, 2465

Butterworth, S., 1930. Theory of filter amplifier. Experimental wireless & the wireless engineer, 7, 536-541.

Casagli N., Catani F., Del Ventisette C. and Luzi G., 2010. Monitoring, prediction, and early warning using ground-based radar interferometry. Landslides, 7, 291-301, doi: 10.1007/s10346-010-0215-y

Cecioni C., G. Bellotti (2010a). Modeling tsunamis generated by submerged landslides using depth integrated equations. Applied Ocean Research, 32, pp. 343-350.

Cecioni C., G. Bellotti (2010b). Inclusion of tsunamis generation into a depth integrated wave propagation model. Natural Hazards and Earth System Sciences, vol. 10, pp. 2259-2268.

Cecioni C., Romano A., Bellotti G., Di Risio M., and De Girolamo P., 2011. Real-time inversion of tsunamis generated by landslides. Nat. Hazards Earth Syst. Sci., 11, 2511-2520, doi:10.5194/nhess-11-2511-2011

Chierici F., Pignagnoli L., and Embriaco D. 2010. Modeling of the hydroacoustic signal and tsunami wave generated by seafloor motion including a porous seabed. Journal of Geophysical Research, 115, C03015, doi:10.1029/2009JC005522.

Corsini, A., Farina, P., Antonello, G., Barbieri, M., Casagli, N., Coren, F., Guerri, L., Ronchetti, F., Sterzai, P., Tarchi, D., 2006. Space-borne and ground-based SAR interferometry as tools for landslide hazard management in civil protection. International Journal of Remote Sensing, 27(12), 2351-2369. doi: 10.1080/01431160600554405.

De Girolamo P., De Berardinis B., Beltrami G.M, Di Risio M., Bellotti G., Capone T. 2011. The Italian activities on tsunami risk mitigation: the operating landslide tsunami early warning system of Stromboli (Aeolian Islands, Italy). In: Proceedings of the 7th International Workshop on Coastal Disaster Prevention. Tokio, Japan, January 26-27, 2011

Di Risio, M., De Girolamo, P., Bellotti, G., Panizzo, A., Aristodemo, F., Molfetta, M.G., Petrillo, A.F. 2009a. Landslide generated tsunamis runup at the coast of a conical island: New physical model experiments. Journal of Geophysical Research, 114, C01009, doi:10.1029/2008JC004858.

Di Risio, M., Bellotti, G., Panizzo, A., De Girolamo, P., 2009b. Three-dimensional experiments on landslide generated waves at a sloping coast. Coastal Engineering, 56(5–6), 659-671, doi:10.1016/j.coastaleng.2009.01.009.

Di Risio, M., De Girolamo, P., Beltrami G.M., 2011 Forecasting Landslide Generated Tsunamis: a Review, in "The Tsunami Threat - Research and Technology", Nils-Axel Morner (Ed.), ISBN: 978-953-307-552-5

Emery, W.J., Thomson, R.E., 2001. *Data analysis methods in physical oceanography*. Elsevier, ISBN 13 978-0-471-46482-2.

Goda, Y., 2000. *Random seas and design of maritime structures*. World Scientific Publishing Co. Pte. Ltd, ISBN 978-981-02-3256-6.

Goring, D.G., 2008, Extracting Long Waves from Tide-Gauge Records, Journal of Waterway, Port, Coastal, and Ocean Engineering, 134(5), 306-312, doi: 10.1061/(ASCE)0733-950X(2008)134:5(306)

Gibbs, J.W. 1899. Fourier series. Nature, 59, pp. 606.

Hamlington B. D., Leben R. R., Godin O. A., Legeais J. F., Gica E., and Titov V. V., 2011. Detection of the 2010 Chilean tsunami using satellite altimetry. Nat. Hazards Earth Syst. Sci., 11, 23912406, doi:10.5194/nhess-11-2511-2011

Langer, H. and Falsaperla, S., 2003. Seismic monitoring at Stromboli volcano (Italy): a case study for data reduction and parameter extraction. Journal of volcanology and geothermal research, 128(1-3), 233-245. doi:10.1016/S0377-0273(03)00257-9.

Leva, D., 2004. Diagramma catena di misura sensore di pressione a Stromboli - Ginostra. Not published presentation (*in Italian*).

McGehee, D. and McKinney, J., 1995. Tsunami detection and warning capability using nearshore submerged pressure transducers - Case study of the 4 October 1994 Shikotan Tsunami. *Proceedings of the 4th International Tsunami Symposium, IUGG, Boulder, Colorado*, pp. 133-144.

Montagna F, Bellotti G., Di Risio M. (2011). 3D numerical modeling of landslide-generated tsunamis around a conical island. Natural Hazards, vol. 58, p. 591-608.

Mofjeld, H.O., 1997. Tsunami detection algorithm. Not published paper (http://nctr.pmel.noaa.gov/tda_documentation.html).

Sammarco P., Cecioni C., Bellotti G., Abdolali A. (2013). Depth-integrated equation for large-scale modelling of low-frequency hydroacoustic waves. Journal of Fluid Mechanics, 722, R6.

Shenoi, B.A., 2006. *Introduction to Digital Signal Processing and Filter Design*. John Wiley and Sons, ISBN 13 978-0-471-46482-2.

Shimizu, K., Nagai, T., Lee, J. H., Izumi, H., Iwasaki, M., Fujita, T., 2006. Development of Real-Time Tsunami Detection System Using Offshore Water Surface Elevation Data. *Proceedings of Techno-Ocean 2006 - 19th JASNAOE Ocean Engineering Symposium, Kobe, Japan*, Paper No. 24.

Smith, S., 1997. *The Scientist and Engineer's Guide to Digital Signal Processing*. California Technical Publishing, ISBN 0-9660176-3-3, (http://www.dspguide.com/, last access 1st July, 2009).

Tinti, S., Pagnoni, F., Zaniboni, F. and Bortolucci, E., 2003. Tsunami generation in Stromboli island and impact on south-east Tyrrhenian coasts. Natuaral Hazards and Earth System Sciences, Vol. 3, pp. 299-309.

Tuah, H., Hudspeth, R.T., 1982. Comparisons of Numerical Random Sea Simulations. Journal of the Waterway Port Coastal and Ocean Division, Vol. 108(4), 569-584, doi: 10.1061/(ASCE)0733-950X(1992)118:6(567).